A Learnable Group-Tube Transform Induced Tensor Nuclear Norm and Its Application for Tensor Completion

Ben-Zheng Li (UESTC)
Xi-Le Zhao, Xiongjun Zhang, Teng-Yu Ji, Xinyu Chen, Michael K. Ng

CSIAM 14 October 2023

Co-author

Xi-Le Zhao

Xiongjun Zhang

Teng-Yu Ji

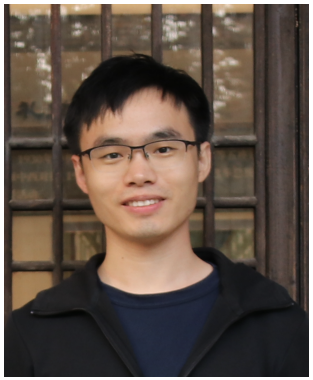

Xinyu Chen

Michael K.Ng

B.-Z. Li, et al., A Learnable Group-Tube Transform Induced Tensor Nuclear Norm and Its Application for Tensor Completion, ***SIAM Journal on Imaging Sciences***, vol. 16, pp. 1370–1397, 2023

Multi-dimensional Data

The rapid advance in imaging technology has given rise to the wide presence of multi-dimensional data (e.g., multi-view, multi-temporal, or multi-modal data):

- color images
- videos
- multispectral/hyperspectral images
- traffic/internet data
- . . .

Degradations

Due to the limitations of imaging devices and environment, multi-dimensional images suffer from degradations, which deteriorate visual quality and hinder subsequent applications.

Tensor completion

The multi-dimensional data can be fully expressed by tensors. Tensor completion refers to the process of inferring missing values from partially observed tensor data.

Low-rankness

For the matrix case (i.e., two dimensional images), the rank is a powerful tool to capture global prior of real-world data.

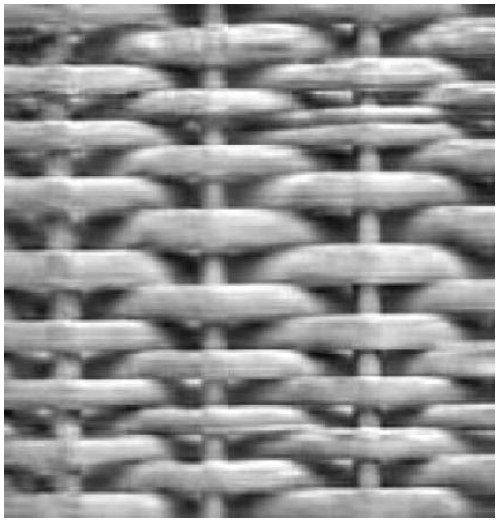

For observed matrix $\mathbf{O} \in \mathbb{R}^{n_1 \times n_2}$, the low-rank matrix completion is mathematically formulated as follows:

$$\begin{aligned} &\min_{\mathbf{X}} \ \operatorname{rank}(\mathbf{X}) \\ &\text{s.t.} \ \ \mathbf{X}_\Omega = \mathbf{O}_\Omega, \end{aligned} \tag{1}$$

where $\mathbf{X}$ is the required matrix and Ω is the index set of the observed elements.

For observed tensor $\mathcal{O} \in \mathbb{R}^{n_1 \times n_2 \times n_3}$, the low-rank tensor completion (LRTC) is mathematically formulated as follows:

$$\begin{aligned} &\min_{\mathcal{X}} \ \operatorname{rank}(\mathcal{X}) \\ &\text{s.t.} \ \ \mathcal{X}_\Omega = \mathcal{O}_\Omega. \end{aligned} \tag{2}$$

The Rank of Tensors

The definition of the rank of tensor is the fundamental problem, which is still an open problem:

- CP decomposition—-CP rank
- Tucker decomposition—-Tucker rank
- Tensor singular value decomposition—tubal rank
- Tensor network decomposition—tensor network rank
- . . .

Tensor-Tensor Product (t-product)

Matrix-Matrix Product:

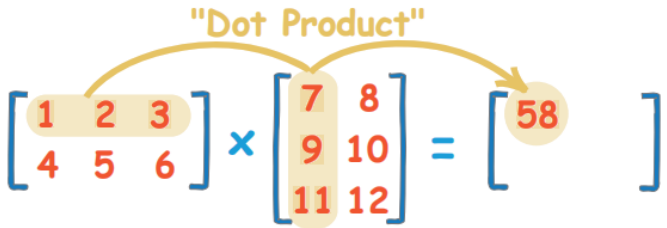

Tensor-Tensor Product:

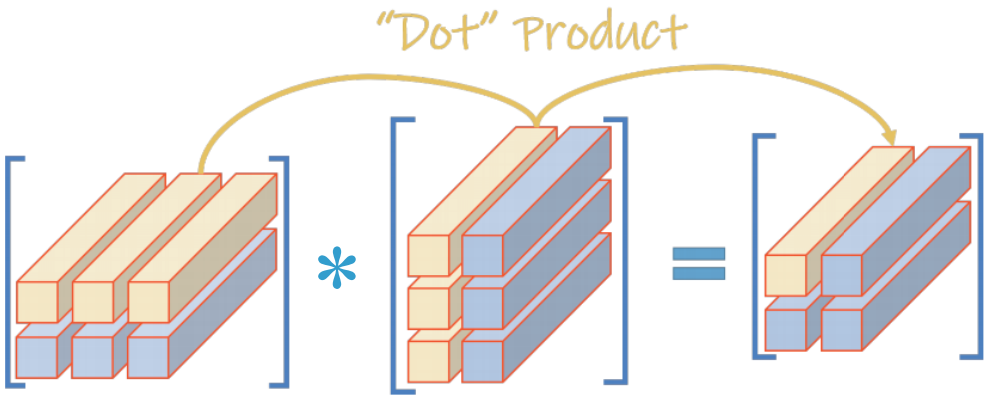

M. E. Kilmer and C. D. Martin, Factorization Strategies for Third-order Tensors, ***Linear Algebra and its Applications***, 2011

Tensor Singular Value Decomposition (t-SVD)

Based on the tensor-tensor product, the tensor singular value decomposition has been emerged as a powerful tool for multi-dimensional image processing:

$$\mathcal{X} = \mathcal{U} * \mathcal{S} * \mathcal{V}^H,$$

where $\mathcal{U}$ and $\mathcal{V}$ are orthogonal tensors, $\mathcal{S}$ is the f-diagonal tensor, and $\mathcal{V}^H$ denotes the conjugate transpose of $\mathcal{V}$.

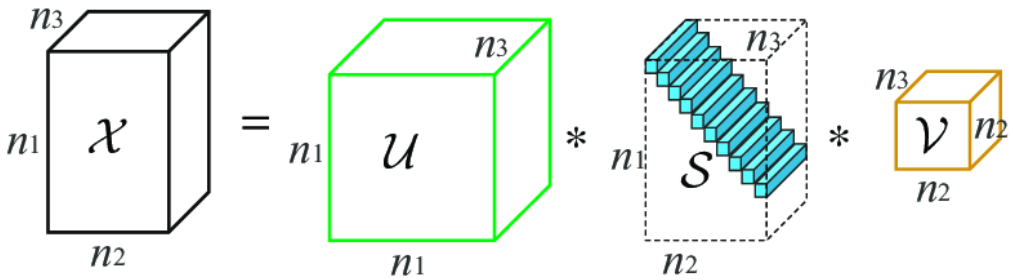

M. E. Kilmer and C. D. Martin, Factorization Strategies for Third-order Tensors, ***Linear Algebra and its Applications***, 2011

Tensor Nuclear Norm (TNN)

Based on t-SVD, the tensor nuclear norm (TNN) was suggested as the convex surrogate to capture the intrinsic structure of the underlying tensor. For $\boldsymbol{\mathcal{X}} \in \mathbb{R}^{n_1 \times n_2 \times n_3}$, TNN is defined as

$$\|\boldsymbol{\mathcal{X}}\|_{\text{TNN}} := \sum_{i=1}^{r} \mathcal{S}(i,i,1),$$

where $\mathcal{S}(i,i,1), i = 1, \cdots, r$ are singular values of $\mathcal{X}$.

Z. M. Zhang, et al., Novel Methods for Multilinear Data Completion and De-noising Based on Tensor-SVD, ***CVPR***, 2014
C. Y. Lu, et al., Tensor Robust Principal Component Analysis with A New Tensor Nuclear Norm, ***IEEE TPAMI***, 2020

TNN-based LRTC

The tensor nuclear norm (TNN) for low-rank tensor completion:

$$\begin{aligned} &\min_{\mathcal{X}} \|\mathcal{X}\|_{\text{TNN}} \\ &\text{s.t. } \mathcal{X}_\Omega = \mathcal{O}_\Omega \end{aligned} \tag{3}$$

The transform-based TNN for low-rank tensor completion:

$$\begin{aligned} &\min_{\mathcal{Z}} \sum_{i=1}^{n_3} \|\mathcal{Z}(:,:,i)\|_* \\ &\text{s.t. } (\mathcal{Z} \times_3 \mathbf{F}_{n_3}^{-1})_\Omega = \mathcal{O}_\Omega, \end{aligned} \tag{4}$$

where $\mathbf{F}_{n_3}^{-1}$ is the pre-defined and unitary inverse DFT.

M. E. Kilmer and C. D. Martin, Factorization Strategies for Third-order Tensors, ***Linear Algebra and its Applications***, 2011

DFT	***Unitary***	***Invertible***	***Non-invertible***
Kilmer *et al.* [2011]	Xu *et al.* [2019]	Kernfled *et al.* [2015]	Jiang *et al.* [2020]
	Song et al. [2020]	Lu *et al.* [2019]	**Kong et al. [2021]**
			Jiang et al. [2021]

M. E. Kilmer and C. D. Martin, Factorization Strategies for Third-order Tensors, ***LAA***, 2011
W.-H. Xu, X.-L. Zhao, and M. Ng, A fast algorithm for cosine transform based tensor singular value decomposition, arXiv:1902.03070, 2019.
G. J. Song, et al., Robust Tensor Completion Using Transformed Tensor Singular Value Decomposition, ***NLAA***, 2020
E. Kernfeld, et al., Tensor-tensor Products with Invertible Linear Transforms, ***LAA***, 2015
C. Y. Lu, et al., Low-Rank Tensor Completion with a New Tensor Nuclear Norm Induced by Invertible Linear Transforms, ***CVPR***, 2019
T. X. Jiang, et al., Framelet Representation of Tensor Nuclear Norm for Third-order Tensor Completion, ***IEEE TIP***, 2020
T. X. Jiang, et al., Dictionary Learning with Low-rank Coding Coefficients for Tensor Completion, ***IEEE TNNLS***, 2021, doi:10.1109/TNNLS.2021.3104837.
H. Kong and Z. C. Lin, Tensor Q-Rank: a New Data Dependent Tensor Rank, ***Machine Learning***, 2021

Correlation of Neighboring Tubes

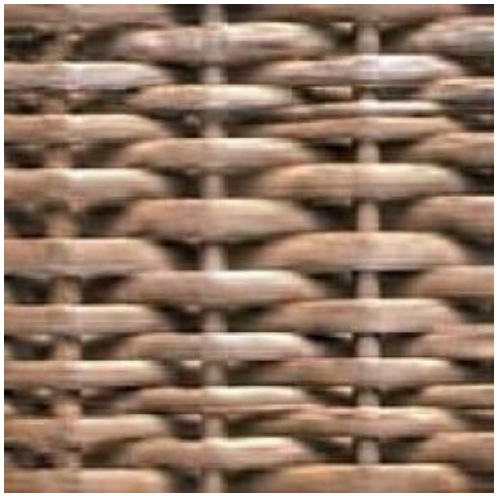

The Group-Tube Transform

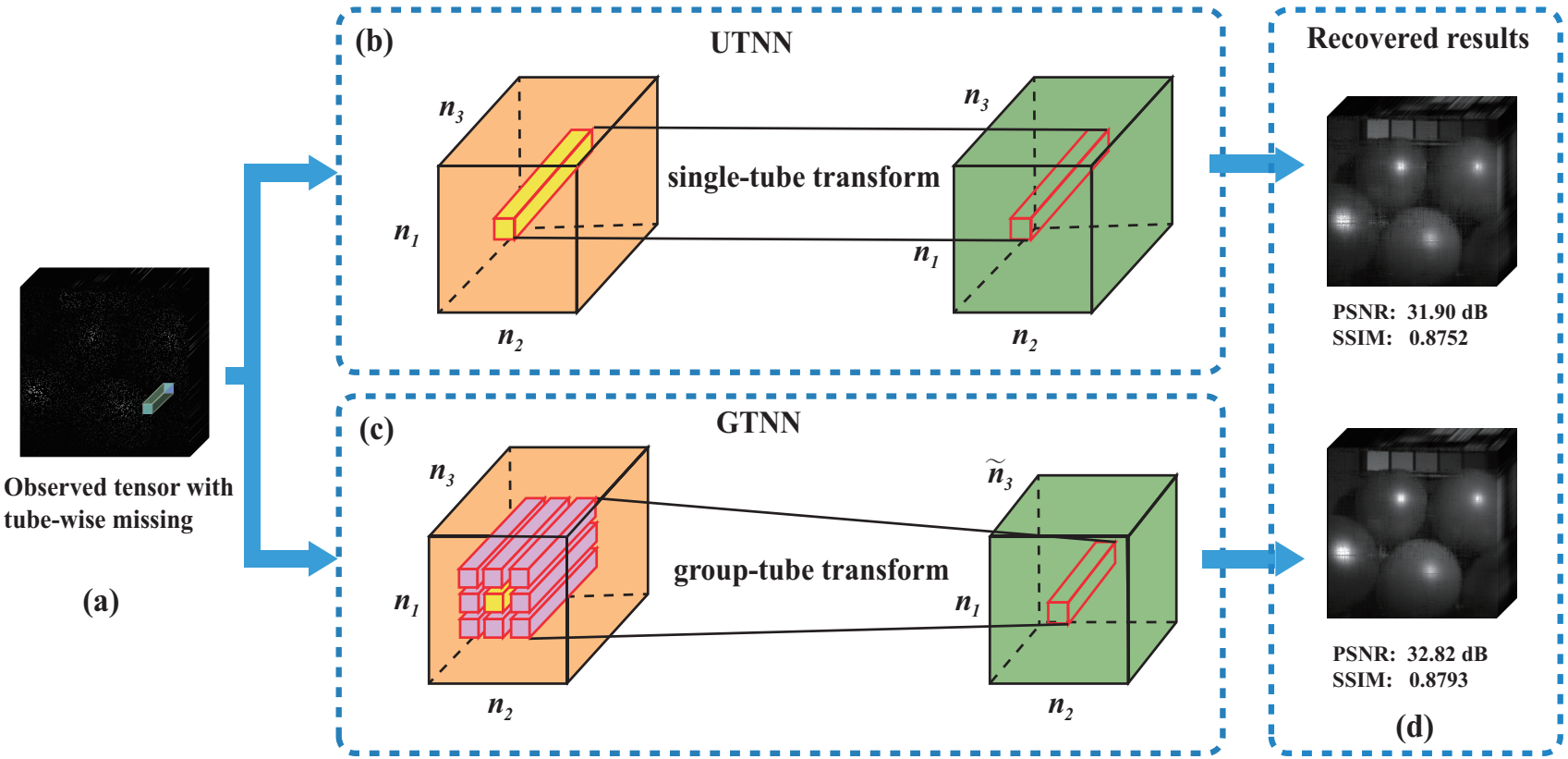

The Group-Tube Transform

The proposed group-tube transform is a separable 3D transform that consists of a 1D spectral/temporal transform (i.e., single-tube transform) and 2D spatial transform.

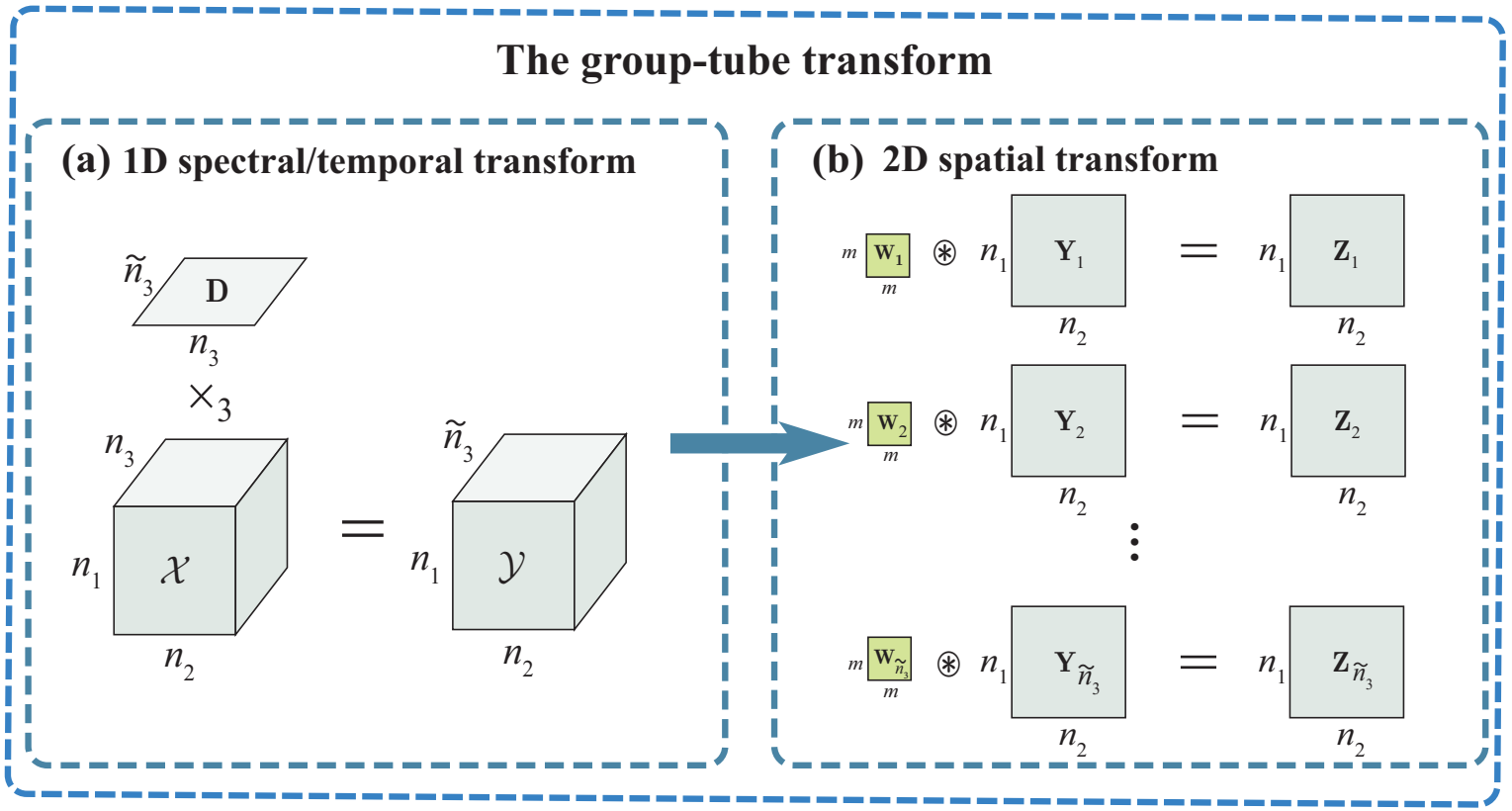

The Group-Tube Transform Induced TNN (GTNN)

Given a target tensor $\mathcal{X} \in \mathbb{R}^{n_1 \times n_2 \times n_3}$, its GTNN is denoted by $\|\mathcal{X}\|_{\text{GTNN}}$. Formally, we have

$$\|\mathcal{X}\|_{\text{GTNN}} \triangleq \sum_{k=1}^{\tilde{n}_3} \|\mathbf{Z}_k\|_*, k = 1, \cdots, \tilde{n}_3,$$

where $\mathbf{Z}_k = \sum_{j=1}^{w} \mathbf{W}_{k,j} \circledast (\mathcal{X} \times_3 \mathbf{D})_k$ is the k-th frontal slice of $\mathcal{Z} \in \mathbb{R}^{n_1 \times n_2 \times \tilde{n}_3}$, $\mathcal{Z}$ is the transformed tensor, and $(\mathcal{X} \times_3 \mathbf{D})_k$ is the k-th frontal slice of $\mathcal{X} \times_3 \mathbf{D}$.

GTNN for LRTC

Given a target tensor $\mathcal{X} \in \mathbb{R}^{n_1 \times n_2 \times n_3}$, the GTNN model for LRTC can be formulated as:

$$\begin{aligned} \min_{\mathcal{X},\mathcal{Y},\mathcal{Z},\mathbf{D},\mathbf{W}_{k,j}} & \sum_{k=1}^{\tilde{n}_3} \|\mathbf{Z}_k\|_* \\ \text{s.t.} \quad & \mathcal{X}_\Omega = \mathcal{O}_\Omega, \mathcal{X} = \mathcal{Y} \times_3 \mathbf{D}^\top, \mathbf{Z}_k = \sum_{j=1}^{w} \mathbf{W}_{k,j} \circledast \mathbf{Y}_k, \\ & \mathbf{D}\mathbf{D}^\top = \mathbf{I}_{\tilde{n}_3}, \left\|\mathbf{W}_{k,j}\right\|_F^2 = 1. \end{aligned} \tag{5}$$

Solving algorithm for GTNN

Introducing auxiliary variables $\mathbf{Q}_{i,j} = \mathbf{W}_{i,j}$, the model (5) can be reformulated as follows by using half quadratic splitting (HQS) tip:

$$\begin{aligned}\min_{\mathcal{X},\mathcal{Y},\mathcal{Z},\mathbf{D},\mathbf{W}_{k,j},\mathbf{Q}_{k,j}} & \sum_{k=1}^{\tilde{n}_3} \|\mathbf{Z}_k\|_* + \frac{\alpha}{2}\|\mathcal{Y} - \mathcal{X} \times_3 \mathbf{D}\|_F^2 + \frac{\beta}{2}\sum_{k=1}^{\tilde{n}_3} \\ & \|\mathbf{Z}_k - \sum_{j=1}^{w} \mathbf{Q}_{k,j} \circledast \mathbf{Y}_k\|_F^2 + \frac{\gamma}{2}\sum_{k=1}^{\tilde{n}_3}\sum_{j=1}^{w} \|\mathbf{W}_{k,j} - \mathbf{Q}_{k,j}\|_F^2 \qquad (6) \\ & + \Phi(\mathcal{X}) + \Psi(\mathbf{D}) + \sum_{k=1}^{\tilde{n}_3}\sum_{j=1}^{w} \Gamma(\mathbf{W}_{k,j}),\end{aligned}$$

where α, β, and γ are positive penalty parameters.

Solving algorithm for GTNN

A proximal alternating minimization (PAM) algorithm for the above model as

$$\begin{cases} \mathcal{X}^{t+1} = \arg\min_{\mathcal{X}}\{g(\mathcal{X}, \mathcal{Y}^t, \mathcal{Z}^t, \mathbf{D}^t, \mathbf{W}_{k,j}^t, \mathbf{Q}_{k,j}^t) + \frac{\rho_1}{2}\|\mathcal{X} - \mathcal{X}^t\|_F^2\}, \\ \mathcal{Y}^{t+1} = \arg\min_{\mathcal{Y}}\{g(\mathcal{X}^{t+1}, \mathcal{Y}, \mathcal{Z}^t, \mathbf{D}^t, \mathbf{W}_{k,j}^t, \mathbf{Q}_{k,j}^t) + \frac{\rho_2}{2}\|\mathcal{Y} - \mathcal{Y}^t\|_F^2\}, \\ \mathcal{Z}^{t+1} = \arg\min_{\mathcal{Z}}\{g(\mathcal{X}^{t+1}, \mathcal{Y}^{t+1}, \mathcal{Z}, \mathbf{D}^t, \mathbf{W}_{k,j}^t, \mathbf{Q}_{k,j}^t) + \frac{\rho_3}{2}\|\mathcal{Z} - \mathcal{Z}^t\|_F^2\}, \\ \mathbf{D}^{t+1} = \arg\min_{\mathbf{D}}\{g(\mathcal{X}^{t+1}, \mathcal{Y}^{t+1}, \mathcal{Z}^{t+1}, \mathbf{D}, \mathbf{W}_{k,j}^t, \mathbf{Q}_{k,j}^t) + \frac{\rho_4}{2}\|\mathbf{D} - \mathbf{D}^t\|_F^2\}, \\ \mathbf{W}_{k,j}^{t+1} = \arg\min_{\mathbf{W}_{k,j}}\{g(\mathcal{X}^{t+1}, \mathcal{Y}^{t+1}, \mathcal{Z}^{t+1}, \mathbf{D}^{t+1}, \mathbf{W}_{k,j}, \mathbf{Q}_{k,j}^t) + \frac{\rho_5}{2}\|\mathbf{W}_{k,j} - \mathbf{W}_{k,j}^t\|_F^2\}, \\ \mathbf{Q}_{k,j}^{t+1} = \arg\min_{\mathbf{Q}_{k,j}}\{g(\mathcal{X}^{t+1}, \mathcal{Y}^{t+1}, \mathcal{Z}^{t+1}, \mathbf{D}^{t+1}, \mathbf{W}_{k,j}^{t+1}, \mathbf{Q}_{k,j}) + \frac{\rho_6}{2}\|\mathbf{Q}_{k,j} - \mathbf{Q}_{k,j}^t\|_F^2\}, \end{cases}$$

where $\rho_l, l = 1, \cdots, 6$ are the proximal parameters.

Theorem

The iterative sequence $\{\mathcal{X}^t, \mathcal{Y}^t, \mathcal{Z}^t, \mathbf{D}^t, \mathbf{W}_{k,j}^t\ \mathbf{Q}_{k,j}^t\}$ *is bounded, and it converges to a critical point of* $g(\mathcal{X}, \mathcal{Y}, \mathcal{Z}, \mathbf{D}, \mathbf{W}_{k,j}, \mathbf{Q}_{k,j})$.

Color Images Completion

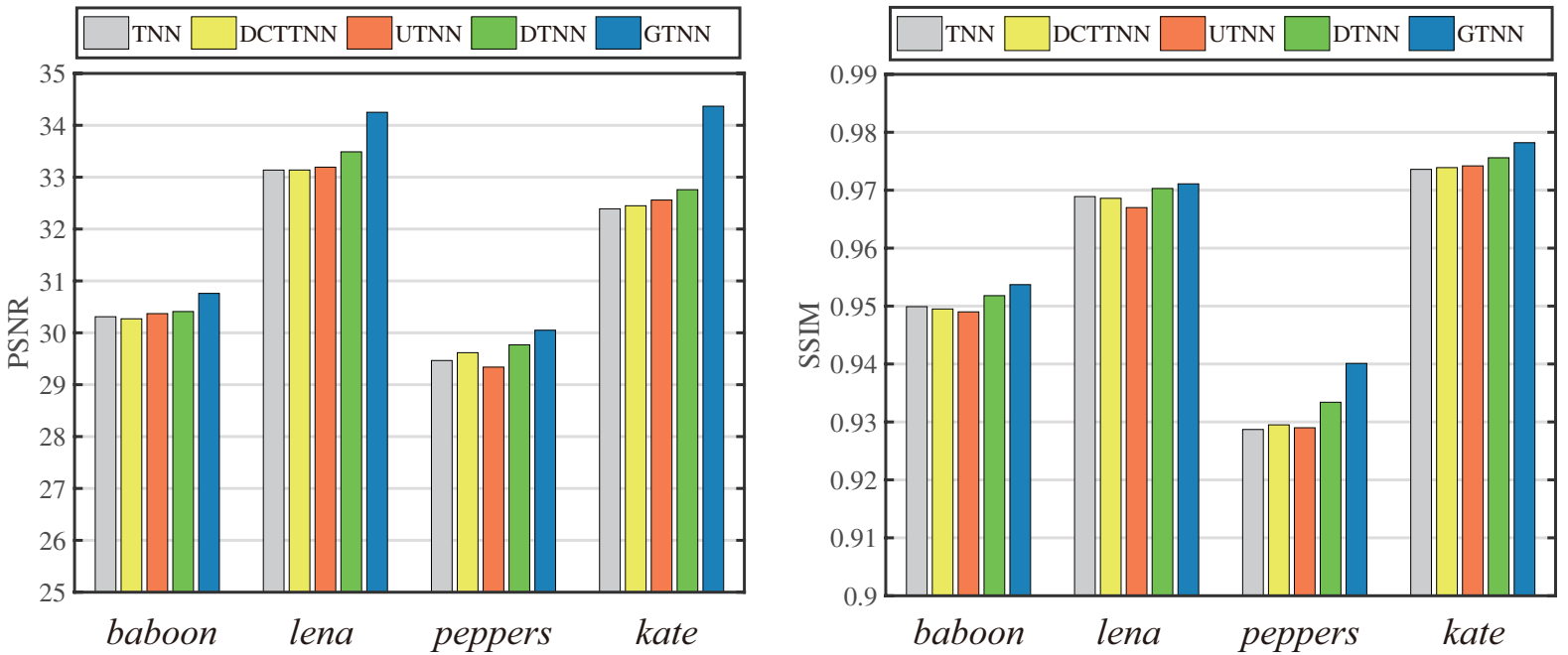

Figure 1: The PSNR and SSIM results of the reconstructed color images by different methods with structural tube-wise missing.

Color Images Completion

Figure 2: The reconstructed color images by different methods with structural tube-wise missing. From top to bottom: *baboon*, *lena*, , and *peppers*, respectively.

Traffic Data Completion

Table 1: The MAPE and RMSE values of the restored traffic speed data *Guangzhou* by different methods with tube-wise missing for different missing rates.

Method	MR=95%		MR=90%		MR=85%		MR=80%	
	MAPE	RMSE	MAPE	RMSE	MAPE	RMSE	MAPE	RMSE
Observed	94.7%	0.476	89.9%	0.464	84.9%	0.450	80.3%	0.439
TNN	63.2%	0.340	29.2%	0.185	13.6%	0.092	11.3%	0.076
DCTTNN	67.5%	0.350	23.6%	0.155	12.4%	0.082	11.2%	0.075
UTNN	45.0%	0.264	14.0%	0.092	11.8%	0.078	10.9%	0.073
DTNN	54.1%	0.305	21.0%	0.142	**11.3%**	0.084	9.7%	0.073
GTNN	**39.9%**	**0.232**	**13.4%**	**0.090**	**11.3%**	**0.075**	**9.2%**	**0.072**

Traffic Data Completion

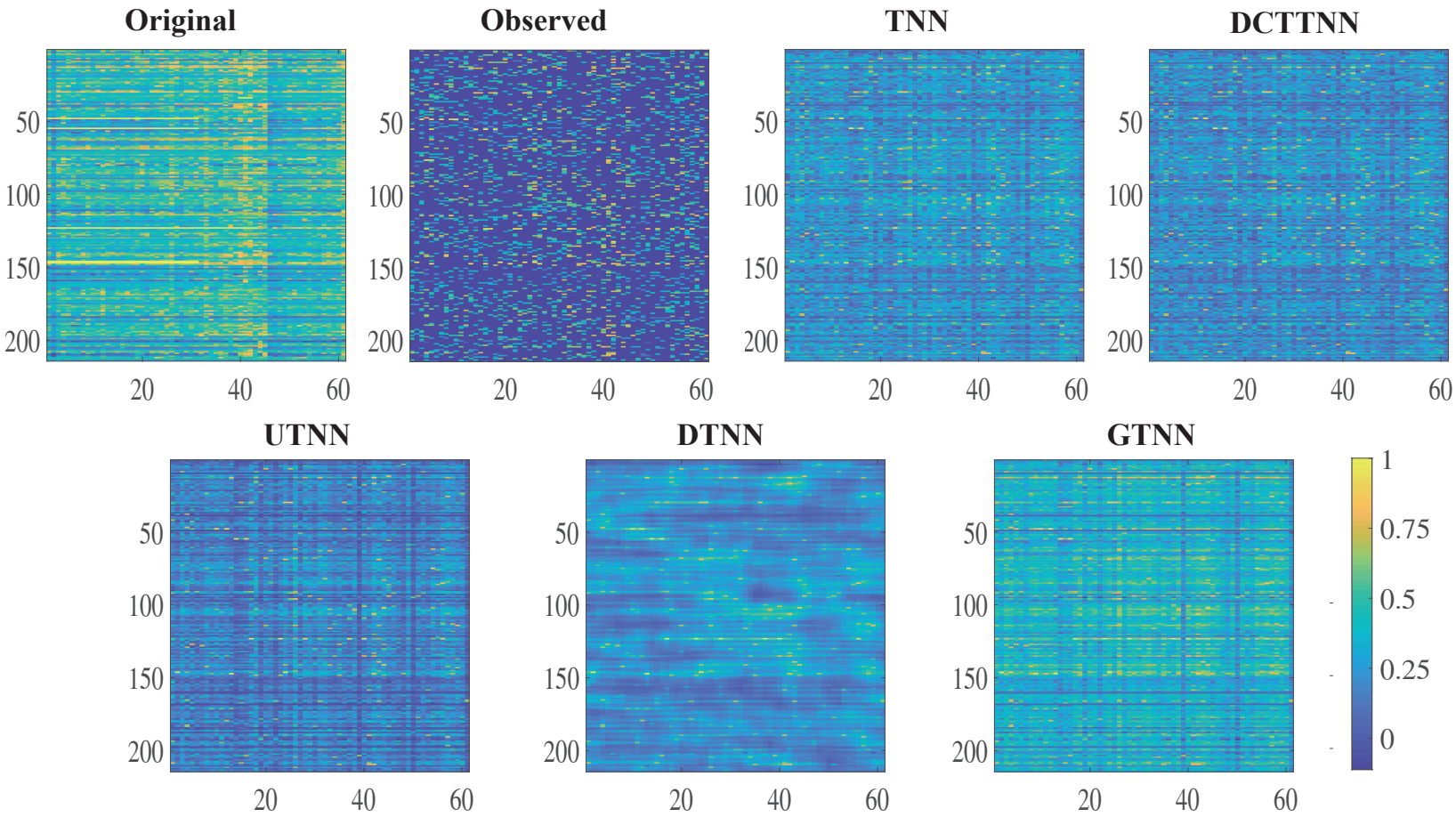

Figure 3: The 100-th frontal slices of the reconstructed traffic speed data *Guangzhou* by different methods with missing rate 80%.

Thank you for your attention!

About me:

Homepage: https://benzhengli.github.io/

Google Scholar: user=pXU2ncUAAAAJ

Github: https://www.researchgate.net/profile/Ben-Zheng-Li